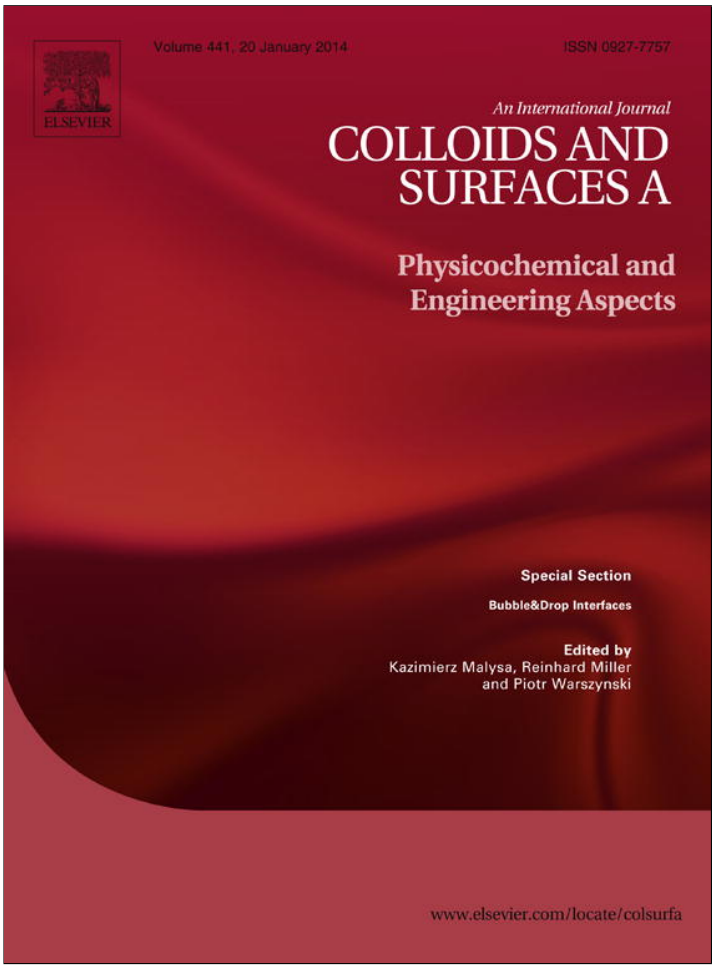

Colloids and Surfaces A: Physicochem. Eng. Aspects 441 (2014) 815–824

Contents lists available at ScienceDirect

Colloids and Surfaces A: Physicochemical and Engineering Aspects

journal homepage: www.elsevier.com/locate/colsurfa

Effect of adding glycerol and Tween 80 on gas holdup and bubble size distribution in an aerated stirred tank

Konstantinos Samaras, Margaritis Kostoglou, Thodoris D. Karapantsios*, Paul Mavros

Division of Chemical Technology, Department of Chemistry, Aristotle University of Thessaloniki, University Box 116, 54124 Thessaloniki, Greece

HIGHLIGHTS

- A non invasive conductance technique measures accurately gas holdup in a STR.
- Gas holdup maximizes at viscosity of 5 mPa s. (non-monotonic viscosity dependence).
- No influence of coalescence/breakage phenomena in the observed phenomena.
- Development of correlations based on the analysis of the results.

GRAPHICAL ABSTRACT

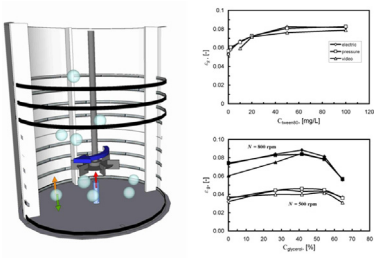

ARTICLE INFO

Article history:
Received 30 October 2012
Received in revised form 14 February 2013
Accepted 18 February 2013
Available online 27 February 2013

Keywords:
Stirred tank
Gas–liquid dispersion
Conductivity
Ring electrodes
Bubble size distribution
Surfactant addition

ABSTRACT

This work presents the results of an experimental parametric study of air-water dispersions in a laboratory scale stirred tank. The quantities monitored are total gas holdup and bubble size distribution. The physical parameters varied, in order to study their effect on the dispersion properties, are liquid viscosity as well as surface tension (static and dynamic) and surface viscoelasticity. Viscosity is varied by adding glycerol whereas surface properties are varied by adding Tween 80. In addition, the effect of the gas flowrate and the stirring rate are studied. Measurements of gas holdup are taken primarily by a non-invasive electrical technique which utilizes ring electrodes flush mounted to the wall. These measurements are verified against simultaneous differential pressure measurements and video images of the instantaneous height of the liquid free surface. Bubble size distributions are estimated analyzing still photographs. In the examined range of parameters, as the concentration of glycerol increases the gas holdup first increases and then decreases going through a peak at 41.6% v/v glycerol (viscosity: 5 mPa s). On the contrary, as the concentration of Tween 80 increases, the gas holdup increases monotonically up to a plateau value at and above 50 mg/l of Tween 80 (static surface tension: 38.3 mN/m). Further analysis of the results indicate no influence of coalescence/breakage phenomena in the observed bubble size distributions.

1. Introduction

Gas–liquid (G–L) stirred tank reactors (STRs) find wide application in the chemical, food and cosmetics process industries, amongst others. Mass transfer between gas and liquid is a rate limiting step in these processes. The mass transfer rates are related to the volumetric gas holdup and the bubble size distribution (BSD), which in turn depend on the local values of these quantities. Gas holdups and BSDs can vary notably regarding mechanical and physical variables, such as agitation speed, gas supply, type of sparger, density, viscosity, salinity and surface tension [1,2].

Through the past four decades, numerous studies have been conducted on aerated STRs concerning the dependence of gas holdup and BSDs from the aforementioned parameters. The techniques used for these measurements are various, and are divided mainly in intrusive and non intrusive. The most widely used intrusive techniques include intrusive conductimetric *pairs of electrodes* [3–5] or *needle type electrodes* [6–10], and *capillary suction probes*

* Corresponding author. Tel.: +30 2310 997772; fax: +30 2310 997759.
E-mail address: karapant@chem.auth.gr (T.D. Karapantsios).

0927-7757/$ – see front matter © 2013 Elsevier B.V. All rights reserved.
http://dx.doi.org/10.1016/j.colsurfa.2013.02.031

Nomenclature

a	function coefficient
B	Baffle width [mm]
b	function coefficient
b_1–b_3	function coefficients
C	Clearance from vessel's bottom [mm]
c_1–c_2	function coefficients
D	Agitator diameter [mm]
$d_{1,0}$	Mean arithmetic diameter [μm]
$d_{1,0e}$	Locally measured mean arithmetic diameter [μm]
$d_{1,0in}$	Mean arithmetic diameter of bubbles leaving the nozzle [μm]
$f(d,x)$	Bubble number concentration density function
$f_o(d)$	Bubble size distribution entering from the nozzle
g	Gravitational acceleration [m/s^2]
g_1–g_2	Functions
g_{1a}–g_{1b}	(sub) Functions
H	Liquid height [mm]
K_{dis}^{app}	Apparent conductance of dispersion [mho]
K_{liq}^{app}	Apparent conductance of liquid phase [mho]
N	Agitator rotation speed [Hz], [rpm]
Q_g	Gas volumetric supply [vvm]
S	Bubble count
T	Tank internal diameter [mm]

Greek symbols

α_1–α_6	function coefficients
γ	Surface tension [mN/m]
Δh	Height difference [mm]
ΔP_h	Hydrostatic pressure difference [Pa]
ε_g	Gas volume fraction [%], [–]
μ	Viscosity [mPa s]
ρ_{liq}	Liquid phase density [Kg/m^3]
σ_{dis}	Conductivity of dispersion [mS/cm]
σ_{liq}	Conductivity of liquid phase [mS/cm]
$\varphi(x)$	Spatial holdup distribution

(CSP) [11–17], while the most popular non intrusive include *tomographic* and *pressure* techniques. The credibility of the intrusive techniques is often disputed in literature, chiefly because of volume exclusion limitations and local stagnation effects. The most widely used non-intrusive techniques are *electrical tomographic techniques* and specifically electrical resistance tomography (ERT) and electrical capacitance tomography (ECT) [18,19]. Less popular are other tomographic techniques, such as *computerized tomography* (CT) [20], and also the *gas disengagement technique* (GDT), in which the free surface of the dispersion is monitored during the disengagement phase [21–24].

Studying the absolute effect of some physical properties, e.g. surface tension, can prove very difficult [25]. For example, most of the surface active substances, even in small concentrations, tend to foam under the intense flow conditions inside a STR. In order to estimate the gas holdup it is common to use empirical equations of the general formulation:

$$\varepsilon_g \propto \left(\frac{\sim {P_g}^A}{V} (u_g)^B \right) \quad (1)$$

where P_g is the required mechanical agitation power, V is the total volume of the dispersion, u_g is the linear velocity of the gas, and A and B are coefficients depending on the coalescence nature of the system [26]. The same holds for the Sauter mean diameter ($d_{3,2}$) and the total gas contact area (α), described for example by Calderbank [27] as:

$$d_{3,2} = 4.15 \left[\frac{Y^{0.6}}{(P_g/V)^{0.4} \rho_l^{0.2}} \right] \varepsilon_g^{0.5} \left(\frac{\mu_g}{\mu_l} \right)^{0.25} + 0.0009 \quad (2)$$

$$\alpha = 1.44 \left[\frac{(P_g/V)^{0.4} \rho_l^{0.2}}{Y^{0.6}} \right] \left(\frac{u_g}{u_t} \right)^{0.5} \quad (3)$$

where γ is the surface tension, μ is the dynamic viscosity of either the liquid ($_l$) or the gas ($_g$) phase, ρ_l is the liquid's density and u_t is the terminal rising velocity of the bubbles. These equations can provide only rough estimations, which some times are very unreasonable. Additionally, they are unsuitable for depicting the mere effect of a single physical property, e.g. liquid viscosity, since they have limited application.

To our knowledge, the isolated effect of liquids' dynamic viscosity on ε_g, and in extension on BSD, has been vaguely studied for STRs and the results have been inconsistent and contradictory [28]. In the same category with G–L STRs fall the bubble columns and the multi-stage agitated contactors (MACs). The scientific literature on this subject is divided into three main categories and a subcategory. The first category found that a viscosity change has no effect on ε_g. This category includes Calderbank [27] who studied 10 different liquids in STRs for μ ranging between 0.5 and 28 mPa s, as well as Hassan and Robinson [29] and Yung et al. [30] who studied water–glycerol and water–glycol solutions up to 2.1 mPa s. Vlaev and Martinov [31] studied two viscoelastic fluids in STRs and also did not observe any notable change in ε_g, a founding supported also by Elgozali et al. [32] for non-coalescing solutions in G-L contactors for μ up to 25.6 mPa s.

The second category of researchers noticed a monotonic increase of ε_g with increasing μ. This category includes Machon et al. [4] who studied water–glycerol solutions in a STR and observed this kind of increase for $\mu < 3.5$ mPa s. Elgozali et al. [32] studied ten Newtonian water solutions for $\mu < 25.6$ mPa s and found that ε_g increased monotonically. Vlaev et al. [3] studied both Newtonian and non-Newtonian solutions in a STR and noticed the same behavior for μ up to 38 mPa s.

The third category of studies observed a monotonic decline of ε_g as viscosity increases. Breman et al. [33] studied in a 9-stage MAC, three liquids with μ ranging from 0.5 to 21 mPa s found a monotonic decrease of ε_g. Zhang et al. [34], also in a MAC, studied sugar solutions with viscosity up to 20 mPa s and found the same pattern. This trend was supported theoretically by Garcia-Ochoa and Gomez [35]. Finally, there is a sub-category that observed a local maximum of ε_g at viscosity values roughly between 2 and 4 mPa s. A local holdup maximum for viscosities around 3 mPa s was found first by Eissa and Schügerl [36], who studied water-glycerol solutions in a bubble column for $\mu < 40$ mPa s. This behavior was explained by the notion that at large viscosities bubble coalescence is promoted through the higher drag forces. Ruzicka et al. [37] found, also in a column, that ε_g reaches a local peak at $\mu = 2$ mPa s. For STRs a local maximum of ε_g was found by Yoshida et al. [38] at 2.6 mPa s, by Machon et al. [4] at 3 mPa s and by Nocentini et al. [39] at 3.7 mPa s.

In the present study, four techniques were used for measuring the total gas holdup and BSD. Specifically, the holdup was measured by: a non invasive electrical technique, a single point pressure measuring technique and a free surface video recording technique, while BSD was measured by static photography. The electrical technique traces were analyzed with the methods of GDT and Fast Fourier Transform, which gave valuable insight about the bubble sizes and the sensitivity of the electrical technique. The parameters studied in the present work are the liquids' surface tension and viscoelasticity (through Tween 80 addition), liquids' viscosity

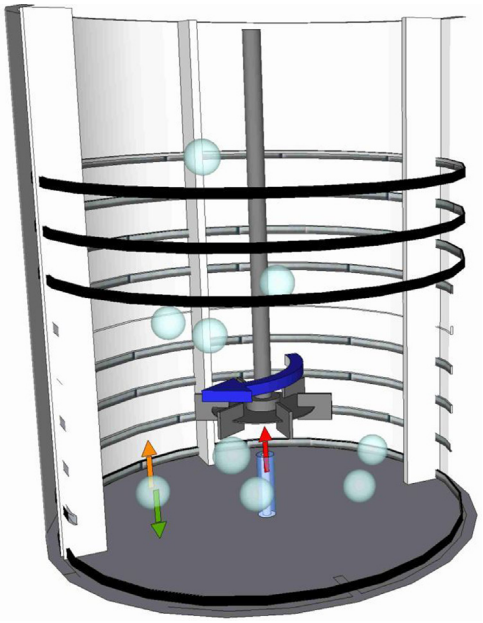

Fig. 1. The experimental apparatus used for the present experiments.

(through glycerol addition), liquids' salinity (through salt addition), impellers' rotation rate and gas flow rate. It must be stressed that adding glycerol in the liquid affects to some extent also the liquid's surface properties. The innovation of this work lies at the last section where an analysis is performed to decouple viscosity effects from surface properties effects.

2. Materials and methods

2.1. Experimental apparatus

The vessel utilized for the role of the STR is a plexiglas cylindrical tank of internal diameter $T = 190$ mm with a curved bottom and four baffles of width $B = T/10$. The impeller used is a Rushton turbine of diameter $D = T/3$ and clearance from the vessel's bottom $C = T/3$. The electrodes are ring-type, wall mounted on the internal periphery of the cylindrical wall. They are made of stainless steel with height 4 mm and width 2 mm. They are equidistantly spaced from each other at 20 mm axial distance, with the first electrode placed at the height of 10 mm from the bottom's center (Fig. 1). Liquid was poured into the vessel up to height $H = T$ from the bottom. Air was fed into the vessel from a nozzle (id = 2 mm) located at the bottom's center. Gas flow rate was measured by a calibrated floating ball rotameter (Fischer–Porter). Gas flow rates are measured in vvm (vessel volume minute), with the vessel volume of liquid always constant at 5 l. Regarding the electrical technique, the maximum axial distance between the far end ring electrodes inside the vessel is 160 mm. Although the combination of these far end electrodes would be expected to give a better total gas holdup it was not chosen because of technical constraints (systematic weak signal). Instead, electrical measurements are taken from a pair of ring electrodes located apart by 140 mm. This separation distance is still large enough to yield the total gas holdup in the vessel.

For the pressure measuring technique an empty glass tube (id = 8 mm) was used, which was submerged into the fluid, behind a baffle into an immobilized test tube, which was attached to the internal wall. The reason for submerging the measuring tube into the test tube is for protection from bubble insertion and suppression of the local pressure fluctuations. The measuring tube is connected to a differential pressure transducer (referenced to ambient pressure – piezoelectric Honeywell 164 pc). For the photographic technique a digital camera Sony DSC–F717 (5 Mpixels) was used shooting at a fixed point, 80 mm from the tanks' bottom center, between two baffles having a focal depth of 20 mm in the radial direction inside the tank, with depth of field ± 15 mm. The free surface video recording was acquired by a portable digital microscope (*Scalar USB Microscope M-1*) between two baffles at 15 fps. Details of the experimental setup are given elsewhere [40].

2.2. Experimental procedure and measurements

An experimental run lasted 80 s and was divided into four stages, namely: *initial calmness* (10 s), with neither agitation nor aeration, which served as the reference value of the pure liquid phase (0% gas fraction), *agitation* (10 s), with agitation in action but no aeration in order to examine the influence of the agitator, *dispersion* (40 s), with both agitation and aeration in action, (this is where the actual measurements are made) and eventually *disengagement* and return to calmness (20 s), where agitation and aeration are both suddenly turned off, where the GDT analysis takes place and which is also used for verification of the initial calmness. The experiments which produced very small bubbles (i.e. high concentration of surfactant or high viscosity), demanded longer dispersion and disengagement times, so they had a total duration of 160 s, with the four stages at 10-10-60-80 s, respectively. The data acquisition frequency was 100 and 200 Hz for the 160 and 80 s experiments, correspondingly.

During the experiments all four techniques were recording simultaneously. The electrical technique has been presented in detail elsewhere [41] for a different application, so only a few essential elements are repeated here. An a.c. carrier voltage of 0.3 V_{RMS} was applied across each electrode pair at a frequency of 25 kHz. This frequency allows suppressing undesirable electrode polarization and capacitive impedance. The response of each electrode pair was fed to an electronic analyzer – demodulator and the analog d.c. output signal of the analyzer was acquired and transformed to digital by a DAS interfaced to a PC (Advantec PCL 818L card). The acquired digital signal was further processed by converting it to apparent conductance K^{app} using a conductance calibration curve based on precise [39] ohmic resistors. Assuming that the ratio of conductivities is equal to the ratio of the apparent conductances (for the pure liquid phase and the dispersion) then:

$$\frac{\sigma_{dis}}{\sigma_{liq}} = \left(\frac{K_{dis}^{app}}{K_{liq}^{app}} \right) \tag{4}$$

where K_{dis}^{app} and σ_{dis} denote the apparent conductance and conductivity of the dispersion, whereas K_{liq}^{app} and σ_{liq} denote the apparent conductance and conductivity of the liquid phase correspondingly. The conductivity measurements were then transformed into air volume fraction (gas holdup), ε_g, using the equation of Maxwell [42]:

$$\varepsilon_g = \frac{3\sigma_{dis}}{\sigma_{dis} + 2\sigma_{liq}} \tag{5}$$

For the point pressure technique the glass tube was submerged to the desirable depth and the data from the pressure transducer were fed to the same DAS of the electrical technique and digitized. Employing measurements at two heights in close proximity (assuming the gas holdup is the same), the gas holdup is resulting from the equation:

$$\Delta P_h = (1 - \varepsilon_g)\rho_{lid} g \Delta h \tag{6}$$

where ΔP_h is the hydrostatic pressure difference, ρ_{liq} is the liquid phase density and Δh the depth difference of the two measuring points (<20 mm).

For the photographic technique, 5–10 still pictures were taken for each run and with the use of a semi-automatic circle identification software [43], about 500 air bubbles were identified in order to avoid biased trends. The pixels were transformed to length via scale photos and finally the diameters of the bubbles were statistically processed in order to produce the BSDs and other statistical descriptors of the distributions.

Finally, the video of the free surface is analyzed frame by frame in order to trace the minimum, maximum and average value of the surface height fluctuation, so that the gas holdup is calculated from the equation:

$$\varepsilon_g = \frac{\Delta h}{H + \Delta h} \tag{7}$$

where Δh represents the height difference of the free surface.

2.3. Series of experiments

Three series of experiments were conducted:

- the *reference* series, where the liquid phase consists of a NaCl aquatic solution of concentration 4.3 mM (resulting in conductivity of 0.5 mS/cm; similar to tap water),
- the series of *viscosity variation* where four concentrations of glycerol in water were employed, and
- the experiments of *surface tension variation* where the nonionic surfactant Tween 80 was employed.

The above are termed as such for simplicity whereas the effect of glycerol to surface properties and the effect of Tween 80 to surface viscoelasticity are dealt with in Section 4.

Also, a fourth series of experiments was conducted using higher concentration of salt (NaCl) or even a different salt ($MgSO_4$). The electrical technique was tuned to tolerate a max conductivity of the liquid at 2 mS/cm, so the maximum concentration of salt could not exceed 15 mM. This max limit was dictated by the need to have high sensitivity in capturing signal undulations during the gas dispersion stage which inevitably was leading to signal saturation at conductivities above 2 mS/cm.

All employed liquid solutions had their conductivity regulated at 0.5 mS/cm by adding the required amount of NaCl. The independent parameters examined in all series are the agitation speed (N) and the air volumetric supply (Q_g). The conditions of all the experiments are shown in Table 1.

The resulted physical properties (surface tension, viscosity and density) of the liquid solutions used at the experiments are presented in Table 2.

Surface tension was measured with a *Lauda TE1/TE2* tensiometer (ring method), the viscosities with an *Anton Paar Physica MCR 301* rheometer (cone-plate method) and the densities with the technique of lecythus. One can observe in Table 2 that the Newtonian solutions of glycerol/water present a slight drop of their surface tension as their viscosity increases. The values of surface tension of these solutions are in good agreement with Machon et al. [4]. Details of the experimental procedures and measurements are given elsewhere [40].

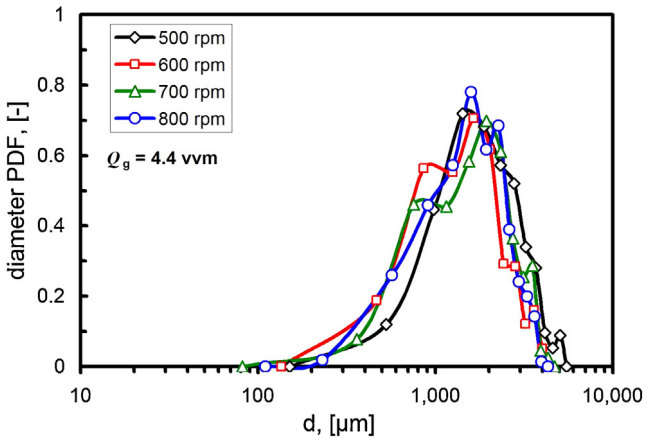

Fig. 2. Probability Density Function of the arithmetic bubble diameter for reference experiments as a function of agitation speed, for a steady aeration supply.

3. Results

3.1. Bubble size distribution

A total of B bubbles are recorded for each experiment and they are distributed in bins according to their size. The diagrams that follow are presented with logarithmic scale on the bubble diameter-axis and the log-normalized probability density function (PDF) on the vertical-axis:

$$y_i = \frac{S_i d_{\mathrm{bin},i}}{\Delta d_{\mathrm{bin}} S} \tag{8}$$

where y_i = the *i-th* value of the PDF function [−], $d_{\mathrm{bin},i}$ = the middle diameter of the *i-th* bin [m], Δd_{bin} = the width of *i-th* bin [m], S_i = the bubble number in the *i-th* bin [−], S = the total bubble number [−].

Fig. 2 presents the BSDs for the reference experiments for all agitation speeds examined, for one aeration supply (4.4 vvm). The similarity among BSDs is apparent, a fact that is also depicted by the average arithmetic bubble diameter ($d_{1,0}$) at Fig. 3a. The same similarity applies also to the other statistical numbers, such as standard deviation, skewness, kurtosis etc. The same invariance of the BSDs and $d_{1,0}$ diameters holds when plotted against aeration supply (Fig. 3b), which leads to the conclusion that for the selected system the bubble size distributions are not affected neither by agitation or aeration.

Table 1
Experiments conducted for the present study.

N (rpm)		500			600			700			800		
Q_g (vvm)		2.4	4.4	5.9	2.4	4.4	5.9	2.4	4.4	5.9	2.4	4.4	5.9
Reference		√	√	√	√	√	√	√	√	√	√	√	√
Surface tension	2				√	√		√	√				
variation, Tween 80	10		√	√	√	√	√	√	√	√	√	√	
(mg/L)	20				√	√		√	√				
	50				√	√		√	√				
	100				√	√		√	√				
Viscosity variation,	26.6		√	√	√	√	√	√	√	√	√	√	
Glycerol (% v/v)	41.6	√	√	√	√	√	√	√	√	√	√	√	√
	54.3	√	√		√	√	√	√	√	√	√	√	
	64.6	√	√		√	√	√	√	√	√	√	√	

Table 2
Physical properties of the liquid phases used for the experiments.

	Reference	Surface tension variation, Tween 80 (mg/L)					Viscosity variation, Glycerol (% v/v)			
		2	10	20	50	100	26.6	41.6	54.3	64.6
Surface tension, γ (mN/m)	71.7	55.0	45.7	42.2	38.3	36.1	68.0	64.0	62.0	60.0
Viscosity, μ (mPa s)	1	1	1	1	1	1	2.5	5	10	20
Density, ρ (kg/m^3)	997	997	997	997	997	997	1067	1106	1140	1167

The dependency of BSDs on surfactant concentration is presented in Fig. 4. As surfactant concentration increases there is a gradual shift of BSDs to the left (smaller diameters) and also a narrowing of the width of the distributions, which is not visually obvious because of the logarithmic scale. Another remark in Fig. 4 is that for surfactant concentration of 2 mg/L the distribution is bimodal which suggests a possible transition concentration from large bubbles (2 mm) to smaller ones (<0.2 mm). For each surfactant concentration, $d_{1,0}$ remains independent of the agitation speed and air supply, as depicted in Fig. 3a and b (triangles). When all the experiments with the same surface tension are averaged then Fig. 5 comes up, representing the increase of the average bubble diameter with increasing surface tension. The red spot at around 50 mN/m corresponding to the 2 mg/L surfactant concentration represents the smaller of the two peak diameters (of the bimodal $d_{1,0}$ distribution).

Fig. 6 presents the BSDs for the experimental series with liquid viscosity variation. Again, the statistical descriptors of BSDs are not affected by the agitation speed and aeration supply (Figs. 3a and b circles and squares). For increasing viscosity up to 5 mPa s the distributions shift to the left (smaller diameters), but for a further increase of viscosity distributions withdraw to the right (larger bubble diameters). The effect of the oscillating BSDs is depicted also on

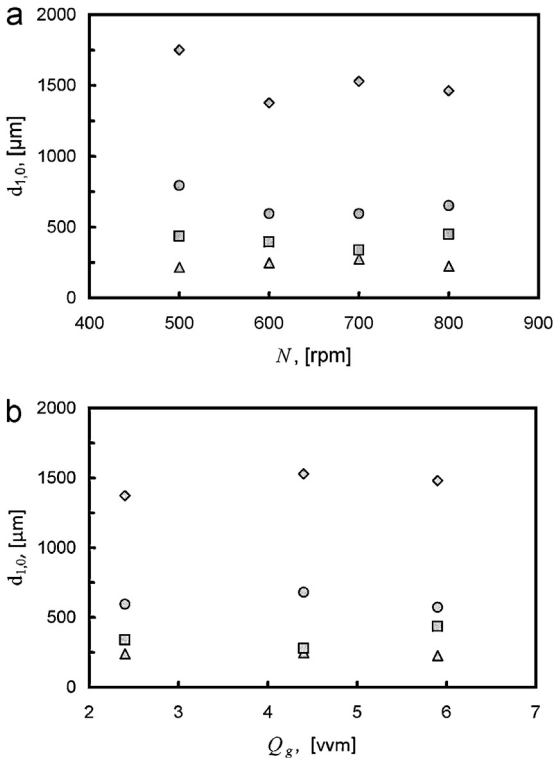

Fig. 3. (a) Mean arithmetic bubble diameters, $d_{1,0}$, as a function of agitation speed for four cases: diamonds = reference with Q_g = 4.4 vvm, circles = 20 mPa s viscosity with Q_g = 2.4 vvm, squares = 5 mPa s viscosity with Q_g = 5.9 vvm, triangles = 10 mg/L surfactant with Q_g = 4.4 vvm. (b) Mean arithmetic bubble diameters, $d_{1,0}$, as a function of air supply for four cases: diamonds = reference with N = 800 rpm, circles = 20 mPa s viscosity with N = 700 rpm, squares = 5 mPa s viscosity with N = 500 rpm, triangles = 10 mg/L surfactant with N = 600 rpm.

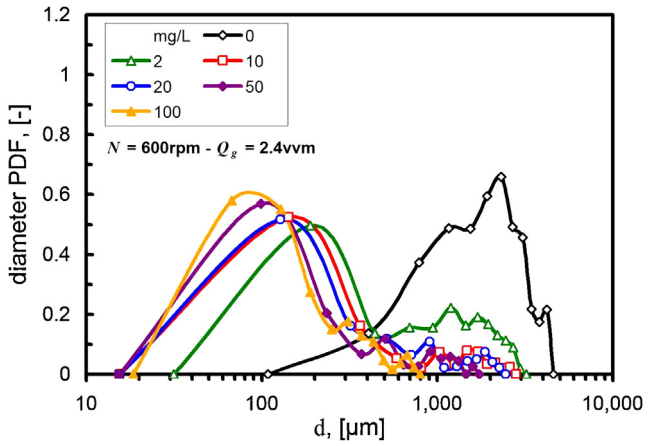

Fig. 4. Probability Density Function of the arithmetic bubble diameter for surface tension variation experiments as a function of surfactant concentration for a combination of agitation speed and aeration supply.

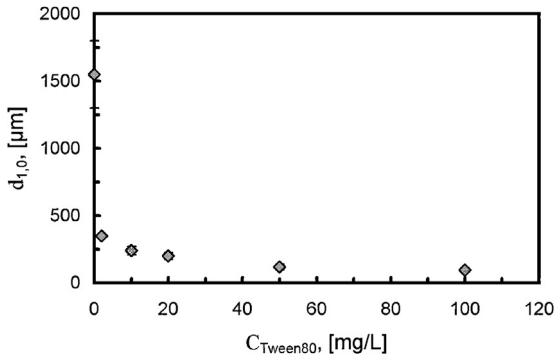

Fig. 5. Mean arithmetic bubble diameters, $d_{1,0}$, toward the surface tension of the liquid phase, caused by the addition of Tween 80.

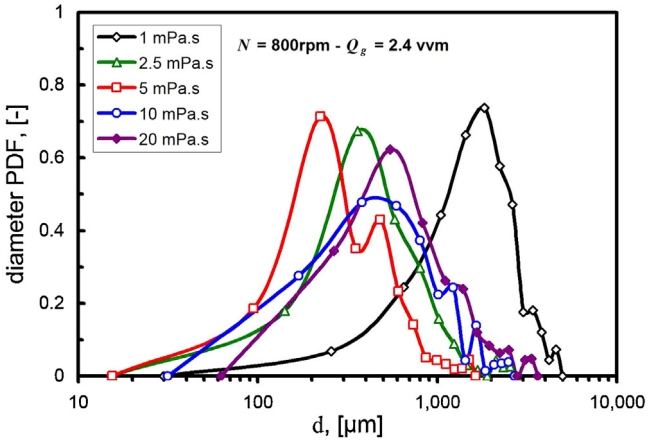

Fig. 6. Probability Density Function of the arithmetic bubble diameter for viscosity variation experiments as a function of liquid phase viscosity for a combination of agitation speed and aeration supply.

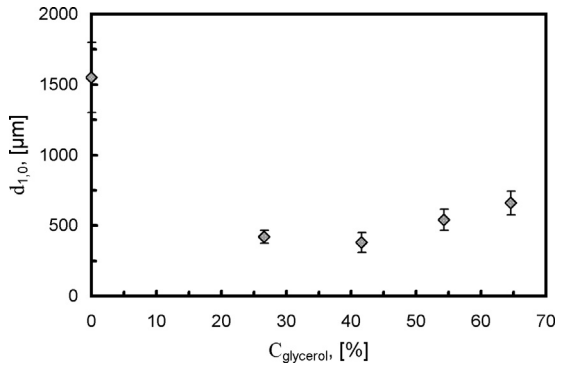

Fig. 7. Mean arithmetic bubble diameters, $d_{1,0}$, as a function of liquid phase viscosity, caused by changing glycerol concentration.

the arithmetic mean diameters (Fig. 7) which presents a minimum for the viscosity value of 5 mPa s.

3.2. Total gas holdup

Fig. 8 presents the values of ε_g for the reference experiments for two agitation speeds and three aeration supplies. The different data markers represent the three measuring techniques: electrical, pressure and free surface video, respectively. It is clear that there is a fair agreement between the three techniques. Also, for steady agitation speed, the dependence of ε_g on Q_g is roughly linear.

Fig. 9 displays the gas holdup for the surface tension variation experiments measured by the three techniques (for one combination of N and Q_g). Also in this case the agreement is fair, with the holdup leveling-off to a plateau value for surfactant concentrations higher than 50 mg/L. This finding combined with the fact that the arithmetic average bubble diameter is not significantly changed above the 50 mg/L, as implied in Fig. 5, this plateau can be considered as the saturation gas-holdup of the system.

For surfactant concentration 10 mg/L, the dependency of ε_g from N for two aeration supplies is presented in Fig. 10. Again, the agreement of the three techniques is fair, with an approximately linear behavior of the total holdup with regards the agitation speed. Fig. 11 shows the total gas holdup against the viscosity, for two agitation speeds and one Q_g, measured with all three techniques. The agreement of the three techniques is still fair. As far it concerns the dependency of ε_g from μ it is apparent that the total holdup presents a local maximum at a viscosity 5 mPa s, regardless the agitation speed.

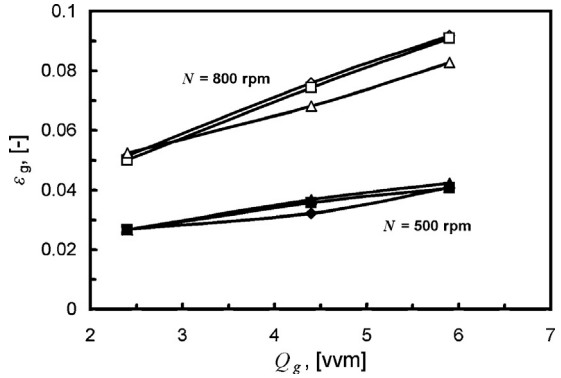

Fig. 8. Total holdups of reference experiments versus the aeration supply, for two agitation speeds, measured by three techniques: diamonds = electric technique, squares = pressure measurement, triangles = free surface video (empty symbols = 800 rpm, filled symbols = 500 rpm).

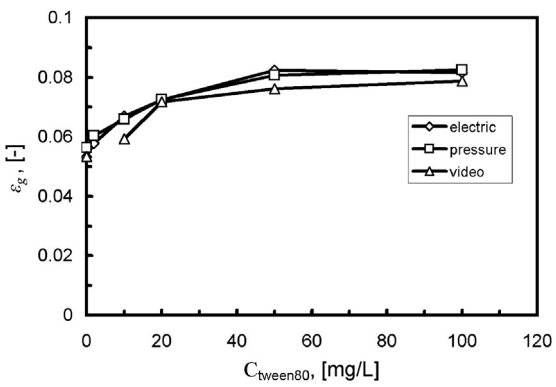

Fig. 9. Total holdups of surface tension variation experiments versus the surfactant concentration, for N = 700 rpm and Q_g = 4.4 vvm, measured by three techniques: diamonds = electric technique, squares = pressure measurement, triangles = free surface video.

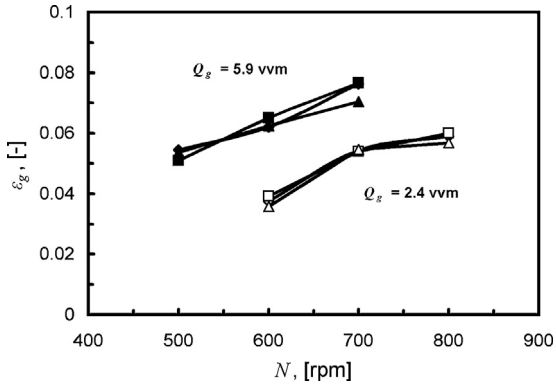

Fig. 10. Total holdups of the 10 mg/L surfactant concentration experiments, for two aeration supplies, measured by three techniques: diamonds = electric technique, squares = pressure measurement, triangles = free surface video (empty symbols Q_g = 2.4 vvm, filled symbols Q_g = 5.9 vvm).

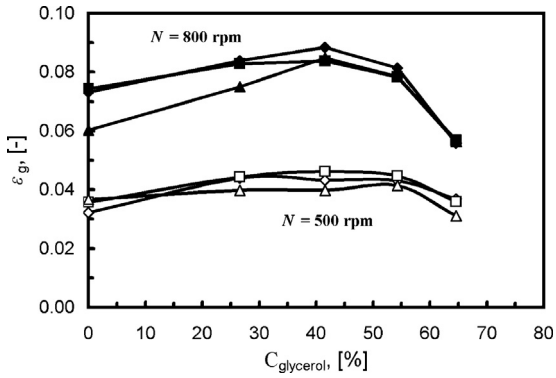

Fig. 11. Total gas holdups of the viscosity variation experiments versus the liquid phase viscosity, for Q_g = 4.4 vvm, measured by three techniques: diamonds = electric technique, squares = pressure measurement, triangles = free surface video (empty symbols N = 500 rpm, filled symbols N = 800 rpm).

4. Problem analysis

Up to this point it was shown that the average holdup in the vessel was measured by three independent techniques with comparable results. Nevertheless, the fluctuations around the average of the signal of the electrical conductance technique are smaller than those of the signals of the other two techniques since they are due only to the discreteness of the bubbles. The other two techniques exhibit additional fluctuations because the flow field

interferes with their measuring principle. The question here is what can be learned from the results of the present work apart from assessing the three holdup measurement techniques. In this respect an attempt is made to describe the occurring phenomena in the present experiment in detail, to simplify their interrelation as suggested by the experimental data and finally, to quantify the experimental results and their relation to the problem parameters always having into mind the relevant literature.

The onset of air injection in the vessel is followed by a transient lasting few seconds and then a steady state is established. This is not a true steady state because of the rotation of the impeller and the non-deterministic motion of bubbles but rather a generalized one, i.e. the average (in time) quantities of interest (like gas holdup or bubble size) does not depend on the period of averaging. Such quantities are customary termed as *stationary* in time-series analysis. The sequence of phenomena occurring in the vessel is: At first the gas leaves the nozzle in the form of bubbles. The size distribution of these bubbles depends, in principle, on the liquid surface tension, viscosity and density, the nozzle diameter and material (dictating the wetting -contact angle- of the nozzle), the gas flow rate and the flow field in the liquid created by impeller. After their departure from the nozzle the bubbles follow trajectories in the vessel which are mainly determined by the liquid flow field and by the buoyancy force on them. The trajectories of the bubbles terminate at the free surface of the liquid. At steady state the total volume of bubbles entering the vessel must be equal to the total volume of bubbles bursting at the free surface. In addition to their motion, bubbles undergo more complicated phenomena such as coalescence and breakage. Both the latter phenomena depend on the turbulent flow intensity and the amount of surfactant in the dispersion. The latter determines the surface tension (static and dynamic) and surface viscoelasticity (interfacial rigidity/mobility) of the bubbles. Having the above general picture of the process, let us quantify the main state variables. The bubble number concentration density function is denoted as $f(x,d)$ where d is the bubble diameter and x is a position vector in the vessel. The corresponding bubble size distribution entering the vessel from the nozzle is denoted as $f_o(d)$. The spatial holdup distribution is denoted as $\varphi(x)$ and it is related to f through the relation.

$$\phi(x) = \frac{\pi}{6}\int_0^\infty d^3 f(x,d)dd \tag{9}$$

Many researchers have studied both experimentally and theoretically the $f(x,d)$ under conditions at which the size distribution is governed by coalescence and breakage. In the present study, the focus is on average or representative quantities of engineering interest. The first quantity of interest is the total holdup, defined as

$$\varepsilon_g = \frac{1}{V}\int_V \phi(x)dx \tag{10}$$

where the integral refers to the whole liquid volume. The second quantity is the number average diameter of the bubbles which is used as the lowest order descriptor of the bubble size distribution. In principle this diameter depends on the spatial variable x and is defined as

$$d_{1,0}(x) = \int_0^\infty df(x,d)dd \Big/ \int_0^\infty f(x,d)dd \tag{11}$$

The quantity $d_{1,0}$ is actually measured in a particular position in the vessel and its values are denoted as $d_{1,0e}$.

After pointing out the state variables and the experimentally measured quantities in the process studied here, let us see now the parameters considered. Of course, only experimentally varying parameters can contribute to the analysis. The geometries of the nozzle and the vessel are fixed so any outcome of the analysis refers to the particular experimental set-up. The density of the liquid can be also assumed fixed (there is actually a small variation due to the glycerol addition to alter the viscosity but the resulting density variation is much smaller than the viscosity variation and as a first approximation can be ignored). So the parameters examined here are the liquid viscosity, the liquid surface tension and the impeller rotation speed. It is stressed that the surface tension is used here just as a way to quantify the effect of surfactant in the liquid (we actually consider only its equilibrium values although it is well known that surfactant dynamics is also important for the phenomena occurring in the vessel). From the above description it is clear that the relations between the measured quantities and the experimental parameters that includes the whole experimental information of the present work are: $d_{1,0e} = g_1(\mu, \gamma, N, Q_g)$ and $\varepsilon_g = g_2(\mu, \gamma, N, Q_g)$.

Let us start with the function g_1. The impeller rotation frequency determines the turbulent intensity in the vessel and this acts on the bubble size in two ways: i) it affects the size $d_{1,0in}$ of the bubbles leaving the nozzle (bubble detachment due to liquid velocity), ii) it determines the measured size $d_{1,0e}$ through the coalescence and breakage processes occurring at the bulk of the liquid. A vast amount of literature exists on the relation between bubble or droplet size and turbulent flow intensity (i.e. N). According to the existing approaches bubble collision rate increases slightly with N but the breakage rate increases abruptly. So a reduction of the bubble size as N increases is predicted by the existing correlations, e.g. Eq. (2). Surprisingly enough the present experimental results show that $d_{1,0}$ is more or less independent from N (i.e. a clear decreasing tendency cannot be detected in the data in Fig. 3a). So as a first approximation it can be considered that $d_{1,0e}$ does not depend on N. The explanation is that for the specific experimental set up and conditions here, the size of the bubbles entering the vessel is smaller than the one predicted by the correlations based on coalescence and breakage, i.e. the bubbles do not undergo coalescence and breakage. This finding differentiates the present work from the related experimental literature in which the bubble size is determined by coalescence and breakage of the bubbles.

Nevertheless, even in the absence of these phenomena there is a spatial non-uniformity of $d_{1,0}$ in the vessel. The buoyancy leads to an increasing value of $d_{1,0}$ as the distance from the bottom of the vessel increases. The point for taking photos in this work is at a median height of the vessel so it is assumed that optical measurements are representative of the bubble size entering the vessel i.e. $d_{1,0e} = d_{1,0in}$. According to the above analysis the function g_1 is the relation between the bubble size leaving the nozzle and the variables μ, γ and Q_g (liquid velocity does not affect the detachment size as suggested by the experimental data). In addition experimental data show independence between $d_{1,0e}$ and Q_g (no effect of gas flow rate on bubble detachment size) so $d_{1,0in} = g_1(\mu,\gamma)$. The bivariate function g_1 must be constructed based on two series of experimental data: one for constant viscosity and several values of surface tension and one for simultaneous variation of viscosity and surface tension. From the first series of data an exponential dependence of bubble size on surface tension results i.e. $g_1 = ae^{b\gamma}$ valid for the pure water viscosity. Keeping in mind that we are not seeking for a fundamental relation but for a way to describe the experimental data of the present work the following tensor product form of the unknown function is assumed: $g_1 = g_{1a}(\mu)g_{1b}(\gamma)$. Using the already known dependence on γ the second series of data can be corrected with respect to surface tension to give the function $g_{1a}(\mu)$. An inverse lognormal distribution is used to fit the corrected data. The experimental second series of data, their correc-

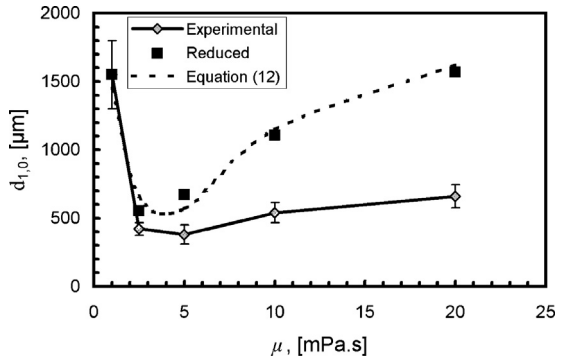

Fig. 12. Mean arithmetic bubble diameters, $d_{1,0}$, as a function of liquid phase viscosity: diamonds = measured by experiments, squares = values reduced to surface tension of 71.7 mN/m, dotted line = best fitting equation.

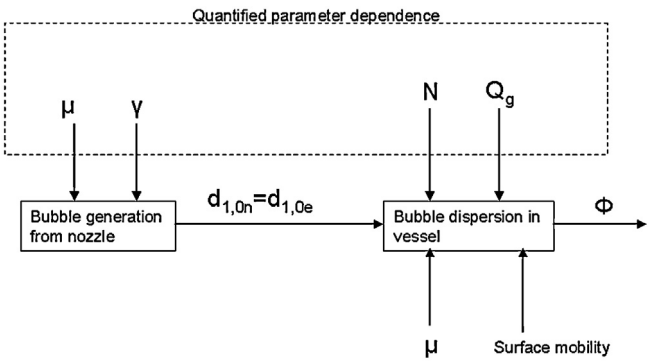

Fig. 13. Flow of information and parametric dependence according to the data analysis procedure followed here.

tion with respect to surface tension (i.e. at reference surface tension of pure water) and the fitting curve are shown in Fig. 12. The final expression for g_1 is

$$d_{1,0} = g_1(\mu, \gamma) = \left(\frac{a_1 - a_2 \exp\left[-\frac{(\ln(\mu/a_3))^2}{a_4} \right]}{1550} \right) a_5 \exp(a_6 \gamma) \quad (12)$$

where $d_{1,0}$ = mean arithmetic diameter [μm], μ = liquid phase viscosity [mPa s], γ = surface tension [mN/m] and the coefficients take the values: $\alpha_1 = 1780$, $\alpha_2 = 1280$, $\alpha_3 = 3.805$, $\alpha_4 = 1.322$, $\alpha_5 = 7.3$ and $\alpha_6 = 0.074$.

The above relation is not fully compatible to the existing theoretical knowledge on bubble sizes generated by orifices. At small gas flow rates and low liquid viscosity the bubble size is determined by buoyancy and surface tension alone so a relation $g_1 = g_1(\gamma)$ is proposed. The theoretical relation between $d_{1,0}$ and γ is weaker than the one suggested by the present experiments. For higher values of viscosity the viscosity starts to influence $d_{1,0}$ but this influence theoretically is associated with an influence of the gas flow rate. The present results reveal an influence of viscosity but not of Q_g on $d_{1,0}$.

The fully coupled problem of spatial and size distribution of bubbles in the vessel can be decomposed for the experimental data examined here to two much simpler problems. The outcome of the first problem which is the size of bubbles leaving the nozzle is an input for the second problem. The information flow in the studied process is shown schematically in Fig. 13. The physics of the second problem which has as outcome the average holdup in the vessel is the following: bubbles with size $d_{1,0}$ and volume flux Q_g enter the vessel. At steady state the holdup is determined from the competition of two motions. The buoyancy motion of the bubbles tries to move them out from the vessel and the fluid motion induced by the impeller try to retain them in the vessel. The variables $d_{1,0}$ and N increase the buoyancy velocity and fluid motion respectively so their increase leads to a decrease (for $d_{1,0}$) or an increase (for N) of the holdup ε_g. The surface tension does not directly affect the problem but its value is associated with the concentration of surfactant which is related to the buoyancy velocity of the bubble. The surfactant concentrations that typically lead to the transition of a mobile liquid surface to an immobile one are small compared to those used here so it is appropriate to separate the data to these referred to mobile surface (absence of surfactant) and these referred to immobile surfaces (presence of surfactant). For a specified value of $d_{1,0in}$, Q_g is proportional to the rate of bubbles entering the vessel so its increase is expected to increase the gas holdup (i.e. $d_{1,0}$ and N determine the isolated bubble behavior and Q_g determines the bubble concentration). From the above, it follows that $\varepsilon_{gi} = g_2(d_{1,0e}, Q_g, N, \mu)$ where the subscript i take the descriptions mobile/immobile. The simplest relation for the function g_2 that can describe the existing experimental data dependence on Q_g and N is the following bi-dimensional polynomial expansion:

$$\varepsilon_g = (a_1 + a_2 Q_g + a_3 Q_g^2) + (b_1 + b_2 Q_g + b_3 Q_g^2) N + (c_1 + c_2 Q_g) N^2 \quad (13)$$

where Q_g = air volumetric supply [vvm], N = agitation frequency [Hz]

A fitting procedure led to the values of the unknown coefficients given in Table 3 where also the average deviation between the data and fitted curves is shown. This fitting procedure can be applied only for the 6 cases for which experiments for all combinations of Q_g and N were made. All the data series refers to mobile bubble surfaces except the second column which refers to immobile surfaces. Many of the coefficients, especially those of higher order terms, are

Table 3
Physical properties of the liquid phase, gas holdup function correlation coefficients and deviation of experimental data from the corresponding equation.

	Reference	Surfactant (10 mg/L)	Viscosity (2.5 mPa s)	Viscosity (5 mPa s)	Viscosity (10 mPa s)	Viscosity (20 mPa s)
μ, (mPa s)	1	1	2.5	5	10	20
γ, (mN/m)	71.7	45.7	68	64	62	60
α_1	0.030643	−0.078739	−0.0005659	−0.034043	0.0083468	−0.027878
α_2	−0.022265	0.028824	−0.0085909	0.0037215	−0.019004	−0.02006
α_3	0.0017057	−0.0026576	0.00054811	−0.00086623	0.0027097	0.0024288
b_1	0.0015296	0.0062557	0.0031948	0.004386	0.0014979	0.014087
b_2	0.0014387	0.000016977	0.0012155	0.0012121	0.0026936	0.00066112
b_3	0	0	0	0	−0.00026872	0
c_1	0	0	0	0	0	−0.00056049
c_2	0	0	0	0	0	−0.000005948
$\Delta(\varepsilon_g)_{ave}$	4.7%	4.8%	1.7%	3.1%	1.9%	8.8%
$\Delta(\varepsilon_g)_{max}$	15.6%	11.8%	4.4%	6.8%	4.2%	14.1%

zero for most cases. The appearance of higher order terms is related to the increase of viscosity. The coefficients a_i, b_i, c_i are according to the above analysis functions of $d_{1,0}$ and μ. But as μ varies, $d_{1,0}$ also varies in a non-monotonic way as it was shown in Fig. 7. This is the reason for the non systematic variation of the coefficients. Taking into account that there is only one value of the coefficients for the mobile surface case and five values for the mobile surface case, the description of the results by equations cannot be continued and need to stop to the combination of Eq. (13), with the coefficients taking values as shown in Table 3. The experimental results follow the expected behavior according to the simple view of the system presented above. The holdup increases with N and Q_g and decreases with $d_{1,0}$. The dependence on μ is complex because μ affects not only directly the buoyancy but also through $d_{1,0in}$.

To this end, appropriate analysis of the process allowed understanding the relation between measured quantities and experimental parameters, the quantification of this relation at the best possible level and its explanation in physical terms. Also in this way the difference between the governing phenomena of the process studied here and the corresponding processes studied in literature is clarified.

5. Conclusions

The present work is an experimental study of the operation of a laboratory-scale aerated vessel using an impeller for gas dispersion with the gas fed through a bottom nozzle. The measured quantities are the total gas holdup in the vessel and the bubble size distribution at a certain height in the vessel. Three different techniques are employed for the total holdup measurement. It was shown that among them the electrical conductance technique performs better since its measurement principle does not interfere with the flow field in the vessel. An extensive analysis of the experimental data reveals the governing phenomena in the particular experimental set-up and the relation between the measured quantities and the physical variables. Empirical correlations are proposed to make this relation explicit. It is shown that literature correlations for bubble size distribution in aerated tanks based on coalescence-breakage competition should not be used without care, since these phenomena do not always determine the bubble size. This is actually the case in the present work.

Acknowledgements

This study is related to the activity of the European network action COST MP1106 “Smart and green interfaces – from single bubbles and drops to industrial, environmental and biomedical applications”, and CM1101 “Colloidal Aspects of Nanoscience for Innovative Processes and Materials”.

References

[1] N. Harnby, M.F. Edwards, A.W. Nienow, Mixing in the Process Industries, Butterworths, London, 1985.
[2] G.B. Wallis, One-Dimensional Two-Phase Flow, McGraw-Hill, New York, 1969.
[3] S.D. Vlaev, M.D. Valena, R. Mann, Some effects of rheology on the spatial distribution of gas hold-up in a mechanically agitated vessel, Chem. Eng. J. 87 (2002) 21–30.
[4] V. Machon, J. Vlcek, A.W. Nienow, J. Solomon, Some effects of pseudoplasticity on hold-up in aerated, agitated vessels, Chem. Eng. J. 19 (1980) 67–74.
[5] S.T. Revankar, M. Ishii, Local interfacial area measurement in bubbly flow, Int. J. Mass. Transfer. 35 (4) (1992) 913–925.
[6] Y. Bao, L. Chen, Z. Gao, J. Chen, Local void fraction and bubble size distributions in cold-gassed and hot-sparged stirred reactors, Chem. Eng. Sci. 65 (2009) 976–984.
[7] M. Barigou, M. Greaves, Gas holdup and interfacial area distributions in a mechanically agitated gas–liquid contactor, Chem. Eng. Res. Des. 74 (1996) 397–405.
[8] A. Bombac, I. Zun, Gas-filled cavity structures and local void fraction distribution in vessel with dual-impellers, Chem. Eng. Sci. 55 (2000) 2995–3001.
[9] A. Bombac, I. Zun, B. Filipic, M. Zumer, Gas-filled cavity structures and local void fraction distribution in aerated stirred vessel, AIChE J. 43 (11) (1997) 2921–2931.
[10] H. Sun, Z-S. Mao, G. Yu, Experimental and numerical study of gas hold-up in surface aerated stirred tanks, Chem. Eng. Sci. 61 (2006) 4098–4110.
[11] M. Barigou, M. Greaves, Bubble-size distributions in a mechanically agitated gas–liquid contactor, Chem. Eng. Sci. 47 (5) (1992) 2009–2025.
[12] M. Barigou, M. Greaves, Bubble size in the impeller region of a rushton turbine, Chem. Eng. Res. Des. 70 (1992) 153–160.
[13] M. Greaves, K.A.H. Kobbacy, Measurement of bubble size distribution in turbulent gas–liquid dispersions, Chem. Eng. Res. Des. 62 (1984) 3–12.
[14] M. Laakkonen, P. Moilanen, J. Aittamaa, Local bubble size distributions in agitated vessels, Chem. Eng. J. 106 (2005) 133–143.
[15] M. Laakkonen, P. Moilanen, V. Alopaeus, J. Aittamaa, Modelling local bubble size distributions in agitated vessels, Chem. Eng. Sci. 62 (2007) 721–740.
[16] S.S. Alves, C.I. Maia, J.M.T. Vasconcelos, A.J. Serralheiro, Bubble size in aerated stirred tanks, Chem. Eng. J. 89 (2002) 109–117.
[17] Y. Nagase, H. Yasui, Fluid motion and mixing in a gas–liquid contactor with turbine agitators, Chem. Eng. J. 27 (1983) 37–47.
[18] M.S. Takriff, A.A. Hamzah, S.K. Kamarudin, J. Abdullah, Electrical resistance tomography investigation of gas dispersion in gas–liquid mixing in an agitated vessel, J. Appl. Sci. 9 (2009) 3110–3115.
[19] M. Wang, A. Dorward, D. Vlaev, R. Mann, Measurements of gas–liquid mixing in a stirred vessel using electrical resistance tomography (ERT), Chem. Eng. J. 77 (2000) 93–98.
[20] Y.-J. Liu, W. Li, L.-C. Han, Y. Cao, H. Luo, M. Al-Dahhan, M.P. Dudukovic, γ-CT measurement and CFD simulation of cross section gas holdup distribution in a gas–liquid stirred standard Rushton tank, Chem. Eng. Sci. 66 (2011) 3721–3731.
[21] M. Cooke, P.J. Heggs, T.L. Rodgers, The effect of solids on the dense phase gas fraction and gas–liquid mass transfer at conditions close to the heterogeneous regime in a mechanically agitated vessel, Chem. Eng. Res. Des. 86 (2008) 869–882.
[22] K.M. Gezork, W. Bujalski, M. Cooke, A.W. Nienow, The transition from homogeneous to heterogeneous flow in a gassed, stirred vessel, Trans. IChemE 78A (2000) 363–370.
[23] A.S. Khare, K. Niranjan, Impeller-agitated aerobic reactor: the influence of tiny bubbles on gas hold-up and mass transfer in highly viscous liquids, Chem. Eng. Sci. 50 (7) (1995) 1091–1105.
[24] K. Sriram, R. Mann, Dynamic gas disengagement, a new technique for assessing the behaviour of bubble columns, Chem. Eng. Sci. 32 (1977) 571–580.
[25] S.P. Evgenidis, N.A. Kazakis, T.D. Karapantsios, Bubbly flow characteristics during decompression sickness: effect of surfactant and electrolyte on bubble size distribution, Colloids Surf. A. Physicochem. Eng. Aspects 365 (2010) 46–51.
[26] G.B. Tatterson, Fluid Mixing and Gas Dispersion in Agitated Tanks, McGraw-Hill Inc., New York, 1991.
[27] P.H. Calderbank, Physical rate processes in industrial fermentation – Part I: the interfacial area in gas–liquid contacting with mechanical agitation, Chem. Eng. Res. Des. 36 (1958) 443–463.
[28] S. Nedeltchev, A. Schumpe, A new approach for the prediction of gas holdup in bubble columns operated under various pressures in the homogeneous regime, J. Chem. Eng. Jpn. 41 (8) (2008) 744–755.
[29] I.T.M. Hassan, C.W. Robinson, Stirred-tank mechanical power requirement and gas holdup in aerated aqueous phases, AIChE J. 23 (1) (1977) 48–56.
[30] C.N. Yung, C.W. Wong, C.L. Chang, Gas holdup and aerated power consumption in mechanically stirred tanks, Can. J. Chem. Eng. 57 (1979) 672–676.
[31] S.D. Vlaev, M. Martinov, Non-uniformity of gas dispersion in turbine-generated viscoelastic circulation flow, Can. J. Chem. Eng. 76 (1998) 405–412.
[32] A. Elgozali, V. Linck, M. Fialova, O. Wein, J. Zahradnik, Influence of viscosity and surface tension on performance of gas–liquid contactors with ejector type distributor, Chem. Eng. Sci. 57 (2002) 2987–2994.
[33] B.B. Breman, A.A.C.M. Beenackers, M.J. Bouma, Flow regimes, gas hold-up and axial gas mixing in gas–liquid multi-stage agitated contactor, Chem. Eng. Sci. 50 (18) (1995) 2963–2982.
[34] L. Zhang, Q. Pan, G.L. Rempel, Liquid phase mixing and gas hold-up in a multistage-agitated contactor with co-current upflow of air/viscous fluids, Chem. Eng. Sci. 61 (2006) 6189–6198.
[35] F. Garcia-Ochoa, E. Gomez, Theoretical prediction of gas–liquid mass transfer coefficient, specific area and hold-up in sparged stirred tanks, Chem. Eng. Sci. 59 (2004) 2489–2501.
[36] S.H. Eissa, K. Schügerl, Holdup and backmixing investigations in cocurrent and countercurrent bubble columns, Chem. Eng. Sci. 30 (1975) 1251–1256.
[37] M.C. Ruzicka, J. Drahos, P.C. Mena, J.A. Teixeira, Effect of viscosity on homogeneous-heterogeneous flow regime transition in bubble columns, Chem. Eng. J. 96 (2003) 15–22.
[38] M. Yoshida, K. Yamagiwa, A. Ito, A. Ohkawa, M. Abe, S. Tezura, M. Shimazaki, Flow and mass transfer in aerated viscous Newtonian liquids in an unbaffled agitated vessel having alternating forward-reverse rotating impellers, J. Chem. Technol. Biotechnol. 76 (2001) 1185–1193.
[39] M. Nocentini, D. Fajner, G. Pasquali, F. Magelli, Gas–liquid mass transfer and holdup in vessels stirred with multiple rushton turbines: water and water–glycerol solutions, Ind. Eng. Chem. Res. 32 (1993) 19–26.
[40] K. Samaras, Study of multiphase flows in stirred tanks, PhD thesis, Department of Chemistry, Aristotle University of Thessaloniki, 2010 (in Greek).

[41] T.D. Karapantsios, M. Papara, On the design of electrical conductance probes for foam drainage applications: assessment of ring electrodes performance and bubble size effects on measurements, Colloids Surf. A 323 (1-3) (2008) 139–148.
[42] J.C. Maxwell, A Treatise on Electricity and Magnetism – Vol. 1, Clarendon Press Series, MacMillan and Co., London, 1873.
[43] X. Zabulis, M. Papara, A. Chatziargyriou, T.D. Karapantsios, Detection of densely dispersed spherical bubbles in digital images based on a template matching technique: application to wet foams, Colloids Surf. A: Physicochem. Eng. Aspects 309 (2007) 96–106.